LAWRENCE
LIVERMORE
NATIONAL
LABORATORY

UCRL-JRNL-224613

Calculation of Radiative Corrections to Hyperfine Splitting in p1/2 States

J. Sapirstein, K. T. Cheng

September 21, 2006

Physical Review A

Updated October 14, 2003

Calculation of Radiative Corrections to Hyperfine Splitting in $p_{1/2}$ States

J. Sapirstein*

Department of Physics, University of Notre Dame, Notre Dame, IN 46556

K. T. Cheng†

University of California, Lawrence Livermore National Laboratory, Livermore, CA 94550

(Dated: September 20, 2006)

Abstract

Techniques to calculate one-loop radiative corrections to hyperfine splitting including binding corrections to all orders have been developed in the last decade for s states of atoms and ions. In this paper these methods are extended to $p_{1/2}$ states for three cases. In the first case, the point-Coulomb $2p_{1/2}$ hyperfine splitting is treated for the hydrogen isoelectonic sequence, and the lowest order result, $\frac{\alpha}{4\pi}E_F$, is shown to have large binding corrections at high Z. In the second case, neutral alkalis are considered. In the third case, hyperfine splitting of the $2p_{1/2}$ state of lithiumlike bismuth is treated. In the latter two cases, correlation corrections are included and, in addition, the point is stressed that uncertainties associated with nuclear structure, which complicate comparison with experiment for s states, are considerably reduced because of the smaller overlap with the nucleus.

PACS numbers: 12.20.Ds, 31.20.Tz, 31.30.Jv

*jsapirst@nd.edu

†ktcheng@llnl.gov

I. INTRODUCTION

Precision theoretical predictions of hyperfine splitting (hfs) in the ground and excited states of alkali atoms and ions requires the understanding of a number of different physical issues. A major challenge is obtaining accurate wave functions, which requires advancements in the atomic many-body problem for atoms beyond lithium. However, even if this problem can be solved to sufficient accuracy, another major problem is the enhanced role of nuclear structure, particularly in highly-charged ions where the electron wave function overlaps the nucleus to a high degree. The distribution of nuclear magnetism is probed, and theoretical uncertainties in this distribution can limit the interpretation of experiment.

In this paper our primary concern is a third kind of physics, the QED correction to the electron magnetic moment. At low Z this is dominated by the Schwinger correction to the lowest-order hfs energy E_F, $\frac{\alpha}{2\pi}E_F$ for s states, $\frac{\alpha}{4\pi}E_F$ for $p_{1/2}$ states, and $-\frac{\alpha}{8\pi}E_F$ for $p_{3/2}$ states [1], but binding corrections can qualitatively change this result. At high Z a perturbative expansion in $Z\alpha$ breaks down and exact calculations using relativistic electron propagators are required. This problem has been studied for s states, and the computational techniques have been developed by a number of groups [2–4]. However, less work has been done on p states, and it is the purpose of this paper to extend our previous calculations to this problem.

Because the basic formalism that we will use has been given in some detail in Ref. [3], we reprise it only briefly in the next section, with most of the discussion devoted to the part of the calculation carried out with free propagators, which differs from our previous work. The following three sections treat the hydrogen isoelectronic sequence, neutral alkalis, and lithiumlike bismuth in turn. In the conclusion, directions for further progress are discussed.

II. COMPUTATIONAL DETAILS

We use an S-matrix approach to calculating both correlation and radiative corrections to hyperfine splitting, which arises from the interaction

$$H_I = -e\int d^3r\, \bar{\psi}(\vec{r},t)\vec{\gamma}\cdot\vec{A}(\vec{r})\psi(\vec{r},t) \tag{1}$$

where

$$\vec{A}(\vec{r}) = \frac{\vec{\mu}\times\vec{r}}{4\pi r^3}F_{BW}(r). \tag{2}$$

Here $\vec{\mu}$ is the magnetic moment of the nucleus and $F_{BW}(r)$ accounts for the distribution of nuclear magnetism, which we model with a simple uniform distribution. More sophisticated distributions can be used, but one of the points of this paper will be that $p_{1/2}$ states are only weakly dependent on this so-called Bohr-Weisskopf effect [5]. We use this distribution only in lowest order, using a point distribution for the QED corrections. Natural units in which $\hbar = c = 1$ are used here.

The formulas for the diagrams of Fig. 1 can be found in our previous work [3, 6–8], and in most cases apply to any state. The exception is the self-energy vertex diagram of Fig. 1b, given by

$$\begin{aligned} E_v &= -4\pi i\alpha \int d^3x\, d^3y\, d^3z \int \frac{d^nk}{(2\pi)^n}\, \frac{e^{i\vec{k}\cdot(\vec{x}-\vec{z})}}{k^2+i\delta}\, \bar{\psi}_v(\vec{x})\gamma_\mu \\ &\quad \times S_F(\vec{x},\vec{y};\epsilon_v - k_0) V(\vec{y}) S_F(\vec{y},\vec{z};\epsilon_v - k_0)\gamma^\mu \psi_v(\vec{z}), \end{aligned} \tag{3}$$

with $V(\vec{y}) = -e\,\vec{\gamma}\cdot\vec{A}(\vec{y})$. This ultraviolet divergent object is rendered finite by subtracting a term with the full bound state propagators S_F replaced with free propagators S_0. This finite term is evaluated in coordinate space in a manner that is valid regardless of the angular momentum of the valence state v. However, the term with free propagators involves more complicated angular momentum issues. It is evaluated in momentum space, and is given by

$$\nu^{\rm SE}(A) = -4\pi i\alpha \int d^3p_2\, d^3p_1 \int \frac{d^nk}{(2\pi)^n}\, \frac{1}{k^2}\, \bar{\psi}_v(\vec{p}_2)\gamma_\mu \frac{1}{\not{p}_2 - \not{k} - m} V(\vec{q}) \frac{1}{\not{p}_1 - \not{k} - m}\gamma^\mu \psi_v(\vec{p}_1), \tag{4}$$

with

$$V(\vec{q}) = ie\vec{\gamma}\cdot\frac{\vec{\mu}\times\vec{q}}{8\pi^3|\vec{q}|^2}. \tag{5}$$

Here $\vec{q} = \vec{p}_2 - \vec{p}_1$ and the energy component of both four vectors p_1 and p_2 is the valence electron energy ϵ_v. The d^nk integration is easily carried out after Feynman parameterization, using $\alpha_1 = \rho x$ for the electron propagator involving p_1, $\alpha_2 = \rho(1-x)$ for the electron propagator involving p_2, and $\alpha_3 = 1-\rho$ for the photon propagator. This parameterization leads to two combinations of $\vec{p}_1$ and $\vec{p}_2$, $\vec{Q}_1 \equiv (1-\alpha_1)\vec{p}_1 - \alpha_2\vec{p}_2$ and $\vec{Q}_2 \equiv (1-\alpha_2)\vec{p}_2 - \alpha_1\vec{p}_1$. Carrying out the d^nk integration then gives

$$\begin{aligned} \nu^{\rm SE}(A) &= -\frac{\alpha}{2\pi}\int_0^1 \rho d\rho \int_0^1 dx \int d^3p_2\, d^3p_1 \bar{\psi}_v(\vec{p}_2) V(\vec{q}) \psi_v(\vec{p}_1) \ln(\Delta_v/m^2) \\ &\quad -\frac{\alpha}{4\pi}\int_0^1 \rho d\rho \int_0^1 dx \int d^3p_2\, d^3p_1 \bar{\psi}_v(\vec{p}_2) N_v \psi_v(\vec{p}_1)(1/\Delta_v), \end{aligned} \tag{6}$$

where an ultraviolet divergent term that cancels with another part of the calculation has been suppressed. In the above,

$$\Delta_v = \rho^2\epsilon_v^2 + \rho(m^2 - \epsilon_v^2) + \alpha_1 \vec{p}_1{}^2 + \alpha_2 \vec{p}_2{}^2 - |\alpha_1\vec{p}_1 + \alpha_2\vec{p}_2|^2 \tag{7}$$

and

$$N_v = \gamma_\mu[(1-\alpha_2)\not{p}_2 - \alpha_1\not{p}_1 + m]\, V(\vec{q})\, [(1-\alpha_1)\not{p}_1 - \alpha_2\not{p}_2 + m]\gamma^\mu. \tag{8}$$

Our momentum space wavefunction is given by

$$u_{n\kappa\nu}(\vec{p}) = \frac{1}{p}\begin{pmatrix} g_v(p)\chi_{\kappa\nu}(\hat{p}) \\ f_v(p)\chi_{-\kappa\nu}(\hat{p}) \end{pmatrix}, \tag{9}$$

where g_v and f_v are upper and lower component wave functions with $v = (n, \kappa)$, and $\chi_{\kappa\nu}$ are spherical spinors. As in our previous work we work with stretched states, which allow us to replace $\vec{\mu}$ with $\mu\hat{z}$. The numerators in $\nu^{\rm SE}(A)$ can then be expressed in terms of a number of operators sandwiched between spherical spinors we denote as T_A through T_J, given by

$$\begin{aligned}
T_A &= \chi^\dagger_{\kappa\nu}(\hat{p}_2)\, \vec{\sigma}\cdot(\hat{z}\times\vec{q})\, \chi_{-\kappa\nu}(\hat{p}_1) \\
T_B &= \chi^\dagger_{-\kappa\nu}(\hat{p}_2)\, \vec{\sigma}\cdot(\hat{z}\times\vec{q})\, \chi_{\kappa\nu}(\hat{p}_1) \\
T_C &= \chi^\dagger_{\kappa\nu}(\hat{p}_2)\, \vec{\sigma}\cdot(\hat{z}\times\vec{q})\, \vec{\sigma}\cdot\vec{Q}_2\, \chi_{\kappa\nu}(\hat{p}_1) \\
T_D &= \chi^\dagger_{-\kappa\nu}(\hat{p}_2)\, \vec{\sigma}\cdot(\hat{z}\times\vec{q})\, \vec{\sigma}\cdot\vec{Q}_2\, \chi_{-\kappa\nu}(\hat{p}_1) \\
T_E &= \chi^\dagger_{\kappa\nu}(\hat{p}_2)\, \vec{\sigma}\cdot\vec{Q}_1\, \vec{\sigma}\cdot(\hat{z}\times\vec{q})\, \chi_{\kappa\nu}(\hat{p}_1) \\
T_F &= \chi^\dagger_{-\kappa\nu}(\hat{p}_2)\, \vec{\sigma}\cdot\vec{Q}_1\, \vec{\sigma}\cdot(\hat{z}\times\vec{q})\, \chi_{-\kappa\nu}(\hat{p}_1) \\
T_G &= \chi^\dagger_{\kappa\nu}(\hat{p}_2)\, \vec{\sigma}\cdot\vec{Q}_1\, \vec{\sigma}\cdot(\hat{z}\times\vec{q})\, \vec{\sigma}\cdot\vec{Q}_2\, \chi_{-\kappa\nu}(\hat{p}_1) \\
T_H &= \chi^\dagger_{-\kappa\nu}(\hat{p}_2)\, \vec{\sigma}\cdot\vec{Q}_1\, \vec{\sigma}\cdot(\hat{z}\times\vec{q})\, \vec{\sigma}\cdot\vec{Q}_2\, \chi_{\kappa\nu}(\hat{p}_1) \\
T_I &= \chi^\dagger_{\kappa\nu}(\hat{p}_2)\, (\hat{z}\times\vec{q})\cdot(\vec{Q}_1 + \vec{Q}_2)\, \chi_{\kappa\nu}(\hat{p}_1) \\
T_J &= \chi^\dagger_{-\kappa\nu}(\hat{p}_2)\, (\hat{z}\times\vec{q})\cdot(\vec{Q}_1 + \vec{Q}_2)\, \chi_{-\kappa\nu}(\hat{p}_1)
\end{aligned} \tag{10}$$

The specific equations are, using the abbreviation $g_v(p_i) = g_i$ and $f_v(p_i) = f_i$,

$$\bar{\psi}_v(\vec{p}_2)V(\vec{q})\psi_v(\vec{p}_1) = \frac{1}{p_2 p_1}(g_2 f_1 T_A + f_2 g_1 T_B) \tag{11}$$

and

$$\begin{aligned}
N_v &= \frac{1}{p_2 p_1}\{(g_2 f_1 T_A + f_2 g_1 T_B)[-2m^2 + 2\epsilon_v^2(1-\rho)^2] \\
&\quad -2\epsilon_v(1-\rho)[(g_2 g_1(T_C + T_E) + f_2 f_1(T_D + T_F)] \\
&\quad +2(g_2 f_1 T_G + f_2 g_1 T_H) + 4m(g_2 g_1 T_I - f_2 f_1 T_J)\}.
\end{aligned} \tag{12}$$

While we have written these operators for a general magnetic quantum number ν, in the stretched state $\nu = j = |\kappa| - 1/2$. We reduce them to functions of p_1, p_2, and the angle between the vectors $\theta = \cos^{-1}(\hat{p}_1 \cdot \hat{p}_2)$ using a device described in Ref. [9], where a rotation allows three of the four angle integrations to be carried out analytically, leaving only the integration over θ to be evaluated numerically. For s states with $\kappa = -1$, this leads to

$$\begin{aligned}
T_A &= p_2 z - p_1 \\
T_B &= p_1 z - p_2 \\
T_C &= p_1 p_2 z(1 + \alpha_1 - \alpha_2) - \alpha_1 p_1^2 - (1 - \alpha_2) p_2^2 \\
T_D &= -p_2 p_1 (z^2 + \alpha_1 - z^2 \alpha_2) + \alpha_1 z p_1^2 + z(1 - \alpha_2) p_2^2 \\
T_E &= p_2 p_1 z(1 + \alpha_2 - \alpha_1) - \alpha_2 p_2^2 - (1 - \alpha_1) p_1^2 \\
T_F &= -p_1 p_2 (z^2 + \alpha_2 - z^2 \alpha_1) + \alpha_2 z p_2^2 + z(1 - \alpha_1) p_1^2 \\
T_G &= p_1^2 p_2 z(1 - \alpha_1^2 - \alpha_2 + 2\alpha_1 \alpha_2) - p_1 p_2^2 z^2 (1 - \alpha_2^2 - \alpha_1 + \alpha_1 \alpha_2) \\
&\quad -\alpha_1(1 - \alpha_1) p_1^3 + \alpha_2(1 - \alpha_2) p_2^3 z - \alpha_1 \alpha_2 p_2^2 p_1 \\
T_H &= p_2^2 p_1 z(1 - \alpha_2^2 - \alpha_1 + 2\alpha_1 \alpha_2) - p_2 p_1^2 z^2 (1 - \alpha_1^2 - \alpha_2 + \alpha_1 \alpha_2) \\
&\quad -\alpha_2(1 - \alpha_2) p_2^3 + \alpha_1(1 - \alpha_1) p_1^3 z - \alpha_1 \alpha_2 p_1^2 p_2 \\
T_I &= 0 \\
T_J &= p_2 p_1 (1 - \rho)(1 - z^2), \qquad (13)
\end{aligned}$$

where a common factor of $\frac{2i}{3}\frac{1}{4\pi}$ is understood. Because we are interested here in $p_{1/2}$ states with $\kappa = 1$ which is opposite in sign to that of the s states, we can evaluate the free propagator term by simply interchanging T_A and T_B, T_C and T_D, and so on. The more complicated formulas for $p_{3/2}$ will be presented elsewhere.

After this reduction a five dimensional integral remains to be evaluated numerically. We were able to achieve high precision with the program CUHRE, part of the CUBA multidimensional integration package [10]. All other parts of the calculation were carried out in the same manner as our s-state work [6–8]. We compress the notation of Ref. [8] as follows. In that work another momentum space integration called $\nu^{\rm SE}(C)$ was associated with the side diagrams of Fig. 1a: here we combine the two into $\nu^{\rm SE}(p) = \nu^{\rm SE}(A) + \nu^{\rm SE}(C)$, with p standing for p-space. Another set of terms were associated with the subtracted parts of the vertex and side diagrams we called $\nu^{\rm SE}(B)$, $\nu^{\rm SE}(D)$, and $\nu^{\rm SE}(E)$, evaluated in coordinate space: here we present only the sum as $\nu^{\rm SE}(x)$. The perturbed orbital terms, $\nu^{\rm SE}(PO)$

are unchanged. For the case of vacuum polarization we also follow the notation of Ref. [8], where the effect was split into a term coming from perturbed orbitals, $\nu^{\rm VP}(PO)$ and a vertex correction $\nu^{\rm VP}(V)$. We now turn to the evaluation of corrections to hyperfine splitting for the three cases described in the introduction.

III. HYDROGEN ISOELECTRONIC SEQUENCE

Precision study of the ground state of the hydrogenic sequence using exact numerical methods is not only crucial for high Z, but is also of value at lower Z where expansions in powers of $Z\alpha$ can be compared with. In Ref. [6] we were able to show agreement with the known parts of the power series and in addition determine the size of the uncalculated higher-order terms, which play a role for muonium hyperfine splitting. Because the nonrelativistic wave function vanishes at the origin for p states, the power series expansion is simpler, being of the form

$$\nu_{2p_{1/2}} = \frac{\alpha}{\pi} E_F \left[\frac{1}{4} + (Z\alpha)^2 \left(a \ln Z\alpha + b\right) + ...\right], \tag{14}$$

in contrast to the s-state expansion, which has a large term linear in $Z\alpha$ and a squared logarithmic term in the next order.

The extraction of coefficients like a and b from the numerical data of exact calculations is always challenging because of the inevitable numerical errors present in that data. These were particularly difficult to control in the present case for two reasons. The first had to do with the slow convergence of the partial wave expansion in both the perturbed orbital and the subtracted vertex terms at low Z. While at higher Z a clear $1/l^3$ behavior was obtained early in the partial wave expansion, at low Z the behavior was still close to $1/l^2$ even at $l = 50$. This leads to an uncertainty of about $0.0001\frac{\alpha}{\pi}E_F$ for $\nu_{2p_{1/2}}$. Also associated with the subtracted vertex term are pole terms, where the Wick rotation encircles more deeply bounded states in one or the other propagators. We use basis set techniques to evaluate these terms, and found some sensitivity to the size of the basis set. For hydrogenic ions, using a basis set with 350 positive- and 350 negative-energy states did give stability at the 0.00001 level. However, for neutral alkalis discussed below, this term was much more difficult to control, in particular forcing us not to treat francium for now.

Our data shown in Table I clearly indicate the presence of the logarithmic term. More interestingly, they also show the presence of a squared logarithmic term which is quite

unexpected. Fitting them to the equation

$$\nu_{2p_{1/2}} = \frac{\alpha}{\pi} E_F \left[\frac{1}{4} + (Z\alpha)^2 \left(A \ln^2 Z\alpha + B \ln Z\alpha + C \right) + ... \right], \tag{15}$$

yields the coefficients

$$A = -0.6(1), \quad B = -0.5(2), \quad C = -2.8(6).$$

In Fig. 2, results computed with these fitted coefficients are seen to agree with those from direct calculations up to $Z = 40$. Without the log-squared term, such good fits are not possible. It would be desirable to have independent confirmation of the existence of the log-squared term, but we are not aware of any such calculation at the present moment.

From Table I and Fig. 2, it can be seen that the deviation of the radiative correction from the Schwinger value increases rapidly as Z increases. As with the s state, a complete reversal of sign is present, taking place around $Z = 40$, and then increasing in magnitude to $-4.095\frac{\alpha}{\pi}E_F$ at $Z = 100$. Thus $p_{1/2}$ states are just as nonperturbative as s states have been shown to be at high Z, and studying hyperfine splitting of p states in highly charged ions probes the same kind of physics as with s states.

IV. NEUTRAL ALKALIS

In a previous work [8] we treated corrections to the hyperfine splitting of the ground states of alkalis, specifically $2s$ for lithium, $3s$ for sodium, $4s$ for potassium, $5s$ for rubidium, $6s$ for cesium, and $7s$ for francium. The Coulomb potential used for the hydrogen isoelectronic sequence is of course no longer an appropriate starting point, and as in Ref. [8] we use a more realistic Kohn-Sham potential modified to give an effective charge of one asymptotically. Calculating QED effects with exact propagators in neutral systems proved quite difficult from a numerical standpoint, and that remains the case for the present calculation of $2p_{1/2}$ for lithium through $6p_{1/2}$ for cesium, with francium proving numerically intractable for now as mentioned above. Extremely fine radial grids with up to 60000 points are required in order to control the numerical Green's functions. Our results are summarized in Table II. As expected, neutral lithium is quite close to the $\frac{\alpha}{4\pi}E_F$ limit, but even though the atoms are neutral, as the nuclear charge increases the feature observed in the hydrogenic case of first a reduction in magnitude and then a sign change is also present. Inclusion of vacuum

polarization works in the opposite direction, so that the total QED effect is reduced, though the change from the Schwinger value as Z increases is still pronounced.

In Table III we present a set of other contributions to the hyperfine splitting. E_F is the lowest-order hfs energy calculated assuming a point magnetic moment, and $\nu^{\rm BW}$ is the shift resulting from the use of a uniform distribution of magnetism in a sphere of radius R. We note that at low Z this effect is very small, as in the nonrelativistic limit $p_{1/2}$ wave functions do not overlap the nucleus. Because of the presence of other electrons we also include the effect of one-photon exchange $\nu^{\rm 1E}$, formulas for which can be found in Ref. [8]. For neutral alkalis this is a very incomplete treatment of correlation, so the agreement of theory with experiment is very poor. Discussion of how this situation can be improved is given in the conclusion.

With the exception of cesium, the precision of the experiments on alkali $p_{1/2}$ states is insufficient to be sensitive to the radiative correction calculated here, although a slight improvement in the lithium measurement would change that situation. However, the accuracy of the cesium experiment [19],

$$\nu_{6p_{1/2}} = 1167.654(60)\ \text{MHz}, \tag{16}$$

which is a 5 ppm experiment, is almost two orders of magnitude greater than the -222 ppm effect found for the QED correction in cesium. Reduction of wave function uncertainties to this level of QED presents a challenge to many-body methods for this atom, which is of considerable interest because of its role in parity nonconservation studies [18]. However, the wave function in this case is sufficiently relativistic that some penetration of the nucleus is present, and the Bohr-Weisskopf effect is 803 ppm, so that it will have to be controlled at the 10 percent level to allow a test of the QED term. This problem would not be present for the $6p_{3/2}$ state, which will be studied in a subsequent work.

V. LITHIUMLIKE BISMUTH

There has been considerable interest in hyperfine splitting in hydrogenlike and lithiumlike bismuth. In the former case, the measurement at GSI [11],

$$\nu_{1s} = 5.0840(8)\ \text{eV}, \tag{17}$$

with a precision of 164 ppm, is in principle adequate to stringently test the QED correction, which is qualitatively changed from the Schwinger value, with the coefficient of $(\alpha/\pi)E_F$ changing from 0.5, a 1162 ppm shift, to -3.5, a -8132 ppm shift. Unfortunately, the size of the Bohr-Weisskopf effect is larger than QED, and uncertainties in it interfere with testing QED. However, as first noted by Shabaev *et al.* [12], carrying out another accurate experiment on the $2s$ state of lithiumlike bismuth allows one to greatly reduce this uncertainty, since the Bohr-Weisskopf effect enters in a similar manner. Specifically, assuming the validity of the QED calculations, one can use the hydrogenic $1s$ result to determine the Bohr-Weisskopf effect, then use that in a lithiumlike $2s$ calculation to make accurate prediction of the 2s hyperfine splitting. Following this suggestion to pin down the Boh-Weisskopf effect, we have, in Ref. [7], calculated the $2s$ splitting to be

$$\nu_{2s} = 0.797\ 15(13)\ \text{eV} \tag{18}$$

While this splitting was measured from the $2s - 2p_{3/2}$ line in an earlier electron beam ion trap (EBIT) experiment [13], the result,

$$\nu_{2s} = 0.820(26)\ \text{eV}, \tag{19}$$

was not accurate enough to test the QED correction. However, a new EBIT experiment [14] is in progress to measure this splitting from the $2s - 2p_{1/2}$ line with more accuracy. In so doing, the $2p_{1/2}$ hyperfine splitting $\nu_{2p_{1/2}}$ may also be resolved, so we present an analysis of this latter splitting incorporating our QED corrections.

In the last columns of Tables II and III, correlation and QED results for the $2p_{1/2}$ hyperfine splitting of lithiumlike bismuth are shown. The correlation part of the calculation is in good agreement with Ref. [15]. The QED effect of -0.193 meV is seen to contribute at a 720 ppm level, so an accurate measurement of the splitting, which we predict to be

$$\nu_{2p_{1/2}} = 264.543\ \text{meV}, \tag{20}$$

should be sensitive to the effect. As with ν_{2s}, this would test the striking qualitative change in sign and order of magnitude of the radiative correction from the Schwinger value. The numbers presented used a Bohr-Weisskopf radius of 5.82 fm determined, as discussed above, by forcing agreement of the hydrogenic $1s$ hyperfine splitting measurement with theory. Because of the reduced overlap with the nucleus of $p_{1/2}$ states, we note that even a 5 percent

change of the 5.82 fm value changes $\nu_{2p_{1/2}}$ by only 0.105 meV, which can be compared to the 1.176 meV change for ν_{2s}. However, there is still significant sensitivity in this case because of the high nuclear charge, as the lower component of the $p_{1/2}$ wavefunction behaves like an s wavefunction. The really dramatic reduction in sensitivity to the Bohr-Weisskopf effect comes when $p_{3/2}$ states are considered, when the same exercise leads to a change of much less than 0.001 meV.

VI. DISCUSSION

We have in this paper applied a numerical method that sums all orders of binding corrections to the QED corrections to hyperfine splitting in $p_{1/2}$ states. While the obvious next step is extending the work to the more difficult case of $p_{3/2}$ states, further research on each of the three cases discussed for $p_{1/2}$ states is called for, and we discuss the cases in turn.

For the point-Coulomb case the most significant problem was numerical in nature. The partial wave expansions can only be carried out to about $l = 50$ with our methods at the present moment, and in some cases the asymptotic region was not quite reached even at the highest partial waves. A similar problem exists when the Zeeman effect is studied with similar methods, and a solution was devised by Beier and collaborators [22]. Rather than subtracting from the vertex diagram only a single term with two free propagators, two more subtractions in which a single Coulomb interaction is present with three free propagators can be made. This dramatically improves the partial wave convergence for the Zeeman effect, and presumably would also allow higher precision to be obtained for the $p_{1/2}$ hyperfine calculation.

For the neutral alkalis less accuracy is needed, as the radiative correction is in general much smaller than other theoretical uncertainties. While one of the main points of this paper is that the Bohr-Weisskopf effect is smaller than for s states, the wave function uncertainties are very difficult to control. The most pressing issue is to gain control over these wave function uncertainties, which is a many-body problem in which it is not necessary to include QED, with the exception that negative energy states must be excluded from intermediate sums over states for certain diagrams. However, at some point one can expect the many body problem will be controlled at a level where QED effects need to be included. At this point a careful combination of QED and MBPT must be made to avoid double counting. Our

calculation of one-photon exchange is done in a QED framework, including negative energy states in intermediate summations and exchange of a transverse photon with retardation: to combine with an MBPT calculation first-order MBPT would have to be subtracted from that term. An interesting issue is what happens for second-order MBPT: it may be necessary at some point to carry out a full two-photon exchange QED calculation for hfs and subtract the MBPT limit. Hopefully the difference would be significantly smaller than the difference for one-photon exchange QED, so that the very difficult project of considering an exact QED calculation of three-photon exchange would not be necessary.

Finally, we have presented results for radiative and correlation corrections to the $2p_{1/2}$ hfs in lithiumlike bismuth. In this interesting case the high nuclear charge plays three roles. The first is improvement of the convergence of the correlation calculation, so that wave function uncertainties are negligible. The second is that the radiative corrections at this high Z qualitatively change from the Schwinger correction result because of the large binding corrections. The last, unfortunately, is that because the $p_{1/2}$ state has a lower component with s-state behavior, there is still sensitivity to the Bohr-Weisskopf effect. However, as noted above, because of the high accuracy experiment on the hydrogenic $1s$ ground state [11], for this ion this uncertainty can be controlled. Regardless, this shows the desirability of doing experiments involving $p_{3/2}$ states, which are basically completely unaffected by this nuclear uncertainty. Because of this we wish to stress the desirability of doing experiments on the hyperfine splitting of states involving $p_{3/2}$ states, for example the ground state of high-Z nitrogenlike ions.

Acknowledgments

We thank Peter Beiersdorfer for helpful discussions regarding the ongoing EBIT experiment. The work of J.S. was supported in part by NSF Grant No. PHY-0451842. The work of K.T.C. was performed under the auspices of the U.S. Department of Energy at the University of California, Lawrence Livermore National Laboratory under Contract No. W-7405-ENG-48.

[1] Stanley J. Brodsky and Ronald G. Parsons, Phys. Rev. **163**, 134 (1967).

[2] H. Persson, S.M. Schneider, W. Greiner, G. Soff, and I. Lindgren, Phys. Rev. Lett. **76**, 1433 (1996).

[3] S.A. Blundell, K.T. Cheng, and J. Sapirstein, Phys. Rev. A **55**, 1857 (1997).

[4] V.M. Shabaev, M. Tomaselli, T. Kühl, A.N. Artemyev, and V.A. Yerokhin, Phys. Rev. A **56**, 252 (1997).

[5] A. Bohr and V.F. Weisskopf, Phys. Rev. **77**, 94 (1950).

[6] S.A. Blundell, K.T. Cheng, and J. Sapirstein, Phys. Rev. Lett. **78**, 4914 (1997).

[7] J. Sapirstein and K.T. Cheng, Phys. Rev. A **63**, 032506 (2001).

[8] J. Sapirstein and K.T. Cheng, Phys. Rev. A **67**, 022512 (2003).

[9] Lars Hambro, Phys. Rev. A **6**, 865 (1972).

[10] T. Hahn, Comput. Phys. Commun. **168**, 78 (2005).

[11] I. Klaft, S. Borneis, T. Engel, B. Fricke, R. Greiser, G. Huber, T. Kühl, D. Marx, R. Neumann, S. Schröder, P. Seelig, and L. Völker, Phys. Rev. Lett. **73**, 2425 (1994).

[12] V.M. Shabaev, A.N. Artemyev, O.M. Zherbtov, V.A. Yerokhin, G. Plunien, and G. Soff, Hyperfine Interaction **127**, 279 (2000).

[13] P. Beiersdorfer, A. Osterheld, J. Scofield, J. Crespo Lopez-Urrutia, and K. Widmann, Phys. Rev. Lett. **80**, 3022 (1998).

[14] P. Beiersdorfer, private communication.

[15] E.Y. Korzinin, N.S. Oreshkina, and V.M Shabaev, Physica Scripta **71**, 464 (2005).

[16] J. Walls, R. Ashby, J.J. Clarke, B. Lu, and W.A. van Wijngaarden, Eur. Phys. J. D **22**, 159 (2003).

[17] W.A. van Wijngaarden and J. Li, Zeit. f. Physik D **32**, 67 (1994).

[18] S.C. Bennett and C.E. Wieman, Phys. Rev. Lett. **82**, 2484 (1999); C.S. Wood *et al.*, Science **275**, 1759 (1997); A. Derevianko and S.G. Porsev, hep-ph/0608178 (2006).

[19] Dipankar Das and Vasant Natarajan, J. Phys. B **39**, 2013 (2006).

[20] E. Arimondo, M. Inguscio, and P. Violino, Rev. Mod. Phys. **49**, 31 (1977).

[21] P. Buck, I.I. Rabi, and B. Senitzky, Phys. Rev. **104**, 553 (1956).

[22] T. Beier *et al.*, Phys. Rev. A **62**, 032510 (2000).

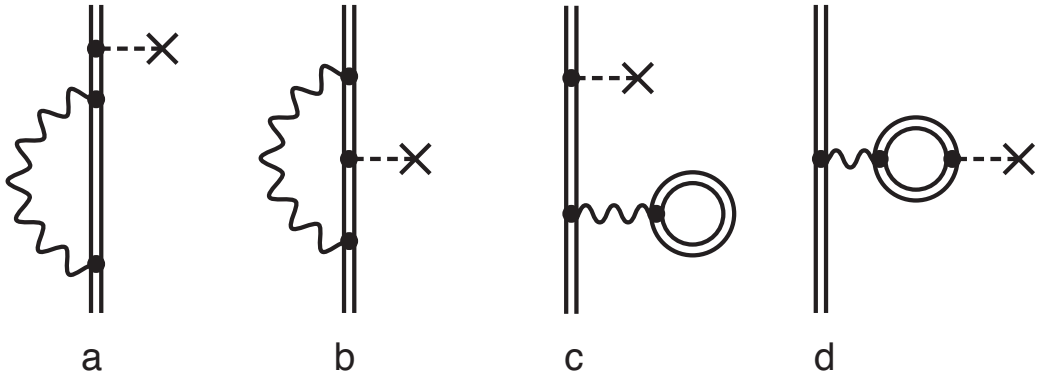

FIG. 1: One-loop self-energy and vacuum polarization diagrams. Dashed lines end with crosses are hyperfine interactions.

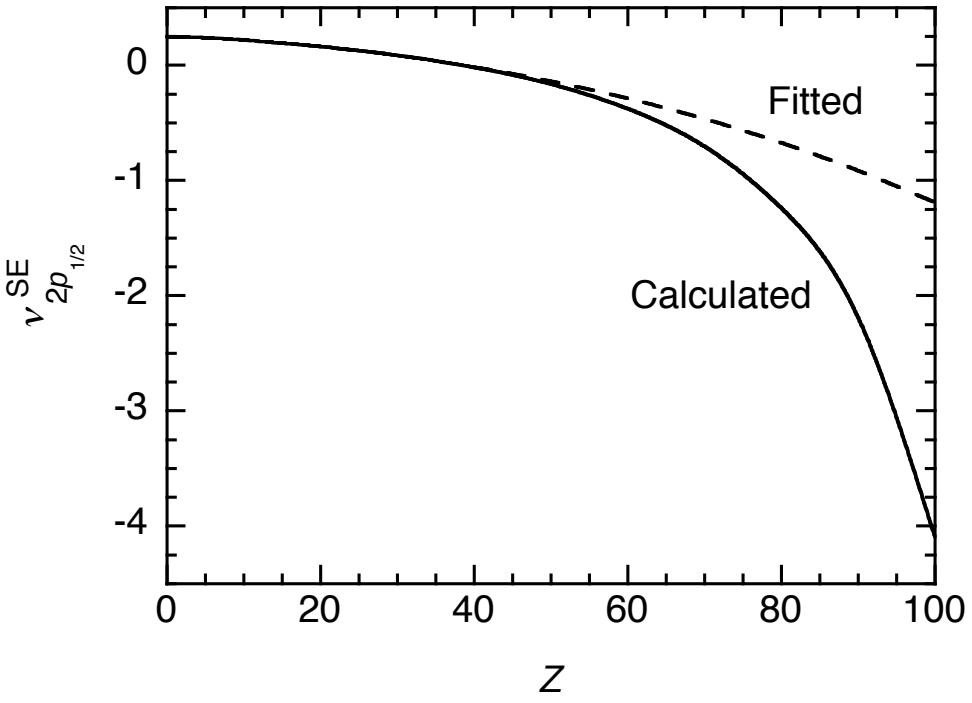

FIG. 2: Self-energy contributions to the $2p_{1/2}$ hfs for hydrogenic ions in units of $(\alpha/\pi)E_F$.

TABLE I: Breakdown of self-energy contributions to hydrogenic $2p_{1/2}$ hfs in units of $\frac{\alpha}{\pi}E_F$.

Z	$\nu^{\rm SE}(PO)$	$\nu^{\rm SE}(p)$	$\nu^{\rm SE}(x)$	$\nu^{\rm SE}$
1	−0.0008	1.1149	−0.8655	0.2487(5)
2	−0.0010	1.1109	−0.8626	0.2474(3)
3	−0.0014	1.1055	−0.8589	0.2452(2)
4	−0.0017	1.0990	−0.8545	0.2427
5	−0.0022	1.0915	−0.8496	0.2397
6	−0.0026	1.0833	−0.8443	0.2364
7	−0.0030	1.0745	−0.8388	0.2327
8	−0.0033	1.0651	−0.8330	0.2288
9	−0.0037	1.0553	−0.8270	0.2246
10	−0.0041	1.0451	−0.8209	0.2202
20	−0.0083	0.9295	−0.7570	0.1642
30	−0.0184	0.8012	−0.6953	0.0876
40	−0.0440	0.6660	−0.6384	−0.0164
50	−0.0999	0.5232	−0.5848	−0.1615
60	−0.2073	0.3685	−0.5365	−0.3752
70	−0.4031	0.1935	−0.4929	−0.7024
80	−0.7574	−0.0191	−0.4606	−1.2371
90	−1.4219	−0.3090	−0.4551	−2.1860
100	−2.7652	−0.7969	−0.5283	−4.0905

TABLE II: Vacuum polarization (VP) and self-energy (SE) contributions to hfs for $np_{1/2}$ states of the alkalis and lithiumlike bismuth. QED is the sum of VP and SE: Units $\frac{\alpha}{\pi}E_F$.

	^{7}Li	^{23}Na	^{39}K	^{87}Rb	^{133}Cs	^{209}Bi^{80+}
$\nu^{\rm VP}(V)$	0.000	0.002	0.006	0.036	0.101	0.313
$\nu^{\rm VP}(PO)$	0.000	0.000	0.002	0.021	0.103	0.641
$\nu^{\rm VP}$	0.000	0.002	0.008	0.057	0.204	0.954
$\nu^{\rm SE}(PO)$	0.000	−0.003	−0.001	−0.059	−0.710	−0.783
$\nu^{\rm SE}(p)$	1.485	5.072	6.628	7.964	8.599	−0.001
$\nu^{\rm SE}(x)$	−1.243	−4.960	−6.830	−7.995	−8.189	−0.480
$\nu^{\rm SE}$	0.242	0.109	−0.032	−0.090	−0.300	−1.264
$\nu^{\rm QED}$	0.242	0.111	−0.024	−0.023	−0.096	−0.310

TABLE III: Correlation and QED contributions to $np_{1/2}$ hfs in the alkalis and lithiumlike bismuth. μ is the nuclear moment in nuclear mageton, I is the nuclear spin, and R is the nuclear radius in Fermi. Units: MHz for the alkalis and meV for lithiumlike bismuth.

	^{7}Li	^{23}Na	^{39}K	^{87}Rb	^{133}Cs	^{209}Bi^{80+}
μ	3.25643	2.21752	0.391466	2.75182	2.58203	4.1106
I	3/2	3/2	3/2	3/2	7/2	9/2
R	3.088	3.825	4.398	5.480	6.206	5.820
E_F	62.447	180.380	49.419	710.533	941.808	267.686
$\nu^{\rm BW}$	0.000	−0.001	−0.000	−0.105	−0.781	−1.143
$\nu^{\rm 1E}$	27.928	−20.757	−6.928	−117.075	−128.380	−1.807
$\nu^{\rm QED}$	0.035	0.046	−0.003	−0.038	−0.210	−0.193
Sum	100.410	159.668	42.488	593.353	812.437	264.543
Expt.	184.04(4)[a]	377.76(52)[b]	57.7(5)[c]	1624.8(32)[d]	1167.654(15)[e]	

[a]Ref. [16].
[b]Ref. [17].
[c]Ref. [21].
[d]Ref. [20].
[e]Ref. [19].